

Finite-time decentralized event-triggered state estimation for coupled neural networks under unreliable Markovian network against mixed cyberattacks

Xiulin Wang(汪修林), Youzhi Cai(蔡有志), and Feng Li(李峰)

Citation: Chin. Phys. B, 2024, 33 (**11**): 110207. DOI: 10.1088/1674-1056/ad7e9a
Journal homepage: http://cpb.iphy.ac.cn; http://iopscience.iop.org/cpb

What follows is a list of articles you may be interested in

On fractional discrete financial system: Bifurcation, chaos, and control

Louiza Diabi, Adel Ouannas, Amel Hioual, Shaher Momani, and Abderrahmane Abbes
Chin. Phys. B, 2024, 33 (**10**): 100201. DOI: 10.1088/1674-1056/ad5d96

Bipartite consensus problems of Lurie multi-agent systems over signed graphs: A contraction approach

Xiaojiao Zhang(张晓娇) and Xiang Wu(吴祥)
Chin. Phys. B, 2024, 33 (**7**): 070204. DOI: 10.1088/1674-1056/ad3dca

Event-based nonfragile state estimation for memristive recurrent neural networks with stochastic cyber-attacks and sensor saturations

Xiao-Guang Shao(邵晓光), Jie Zhang(张捷), and Yan-Juan Lu(鲁延娟)
Chin. Phys. B, 2024, 33 (**7**): 070203. DOI: 10.1088/1674-1056/ad3dcb

Target layer state estimation in multi-layer complex dynamical networks considering nonlinear node dynamics

Yayong Wu(吴亚勇), Xinwei Wang(王欣伟), and Guo-Ping Jiang(蒋国平)
Chin. Phys. B, 2024, 33 (**4**): 040205. DOI: 10.1088/1674-1056/ad20d7

Finite-time H_∞ filtering for Markov jump systems with uniform quantization

Jingjing Dong(董敬敬), Xiaofeng Ma(马晓峰), Xiaoqing Zhang(张晓庆), Jianping Zhou(周建平), and Zhen Wang(王震)
Chin. Phys. B, 2023, 32 (**11**): 110202. DOI: 10.1088/1674-1056/acedf5

Finite-time decentralized event-triggered state estimation for coupled neural networks under unreliable Markovian network against mixed cyberattacks

Xiulin Wang(汪修林), Youzhi Cai(蔡有志), and Feng Li(李峰)†

School of Electrical and Information Engineering, Anhui University of Technology, Maanshan 243032, *China*

(Received 17 July 2024; revised manuscript received 4 September 2024; accepted manuscript online 24 September 2024)

This article investigates the issue of finite-time state estimation in coupled neural networks under random mixed cyberattacks, in which the Markov process is used to model the mixed cyberattacks. To optimize the utilization of channel resources, a decentralized event-triggered mechanism is adopted during the information transmission. By establishing the augmentation system and constructing the Lyapunov function, sufficient conditions are obtained for the system to be finite-time bounded and satisfy the H_∞ performance index. Then, under these conditions, a suitable state estimator gain is obtained. Finally, the feasibility of the method is verified by a given illustrative example.

Keywords: Markov jump systems, coupled neural networks, decentralized event-triggered mechanism, finite-time state estimation

PACS: 02.30.Yy, 07.05.Mh, 02.50.Ga **DOI:** 10.1088/1674-1056/ad7e9a

1. Introduction

In recent years, neural networks (NNs) have been applied more and more widely in the physical layer.[1] NNs can be used to analyze a large number of particle collision data and extract useful information from it. It can also analyze the structure and properties of materials, and predict the physical properties of materials such as hardness and electrical conductivity. In addition, NNs can be used as an effective modeling tool for some physical systems that are difficult to model with traditional analytical methods. More and more reports have been published to investigate the application of NNs in physics.[2–4] NNs can also handle distributed information by adjusting the connection relationship between internal nodes. It is used in pattern recognition, signal processing, knowledge engineering, optimization combination, robot control, and so on.[5–9] Coupled neural networks (CNNs) are a special type of NNs structure, which unique coupling mechanism significantly improves the performance of NNs. Through this coupling mechanism, feedback connections are introduced between different layers of the NNs, so as to realize the transmission of physical signals and data analysis. Compared with traditional NNs, CNNs have obvious advantages in model representation, information interaction, and cooperative processing, robustness, and interpretability.[10,11]

In addition, there is an increasing number of studies on issues such as synchronization control, state estimation, and target detection of CNNs.[12–15] State estimation, as one of the main issues in the study of CNNs, is of great significance in robot control, aerospace, and other areas, to achieve intelligence and automation. However, in the study of the state estimation problem for CNNs, the channel resources for transmitting information are usually limited. To rationalize the use of limited channel resources, an event-triggered mechanism (ETM) was proposed in Ref. [16]. Compared with the time-triggered mechanism, there are no unnecessary transmissions and calculations due to periodicity, and the trigger threshold conditions can be set artificially to reasonably select the information to be transmitted. Therefore, the ETM was utilized to deal with the state estimation problem of CNNs has become a hot research topic in recent years.[17–19] Constructed time-delayed event-triggered estimators in order to achieve energy-efficient estimation of CNNs and a more flexible dynamic ETM based on the original static ETM by setting the threshold parameter as a variable was adopted in Ref. [20]. Besides, the authors considered the characteristics of multiple network nodes in Ref. [21], the use of decentralized event-triggered mechanism (DETM) made the operation of CNNs more flexible. The calculation and communication of the node will be triggered only when the state of the node changes, which greatly reduces the amount of calculation and saves communication bandwidth.

With the continuous development of the network, network security problems have gradually become apparent. Cyberattacks have emerged as a serious threat to network security and have become a focal point of research. These attacks include denial-of-service (DoS) attacks, deception attacks, and other kind of attacks. Generally, DoS attacks occur when attackers send numerous false service requests that are inaccessible to the target user, resulting in channel blockage.[22] The probability of DoS attacks based on the Bernoulli sequence

†Corresponding author. E-mail: fengli4131@gmail.com

© 2024 Chinese Physical Society and IOP Publishing Ltd

was discussed in Ref. [23]. In Ref. [24], deception attacks were essentially a form of cyberattack that deceives trust. The attacker exploited the flaws in the authentication mechanism and disguised himself as a trusted party to communicate with the victim and ultimately collect information or launch further attacks. The authors designed state estimators based on partial nodes of the system under random deception attacks, where Bernoulli sequences were used for modeling and the attack signals were norm-bounded. In the above-mentioned reference that introduced cyberattacks, only the impact of a single cyberattack on the system was considered, and the Bernoulli sequence was used to model cyberattacks.[25–27] However, in practice, it is not sufficient to consider only one type of cyberattack, and when modeling cyber attacks using Bernoulli sequences, it is only possible to indicate whether or not an attack has been suffered, switching between the two modes of attack and normal. This approach is inappropriate when there are multiple attacks. Therefore, mixed cyberattacks were modeled using Markov processes, which can better reflect the dynamic nature of attacks.[28–30] When subjected to multiple attacks, systems can randomly switch between normal operation and different attack modalities. Markov process modeling allows for a more accurate representation and analysis of network attacks based on different modes and transition probabilities, enabling predictions about future attacker behavior. The superiority of Markov process modeling attracted attention from researchers and was applied to study and solve various problems.[31–33] However, there has been no research to date using this approach to model mixed cyberattacks. This article aims to fill that gap by focusing on this topic.

The above-mentioned problems of state estimation for studying CNNs are in the infinite time horizon. However, in practical engineering applications, due to time, resource, and other constraints, it is not appropriate to consider the asymptotic stabilization properties of the system in infinite time, and it is necessary to ensure that the state of the system achieves the desired effect within the specified constraints, hence, the finite-time state estimation problem became a topic of wide interest in recent years.[34–37] It is due to the application of this finite-time boundedness that the study of the above problem in finite time is very meaningful and necessary.

Inspired by the above analyses, this article mainly studies the finite-time state estimation of coupled neural networks using DETM under randomly occurring cyberattacks. There are the main contributions of the article.

(i) Unlike existing research CNNs that use the Bernoulli distribution to model mixed cyberattacks, this article uses a Markov process to model the mixed cyberattacks suffered by CNNs during data transmission. The mixed cyberattack model based on the Markov process can be updated and adapted in real time to adapt to dynamically changing cyberattacks. The mode transition probabilities therein can be used to explain the relationship between different attack behaviors, enhancing the interpretability of the mixed cyberattacks model.

(ii) Aiming at the finite-time state estimation problem of CNNs, an effective DETM is established, and an event-triggering-based state estimator design method is given, which can effectively reduce the occupation of the channel bandwidth and achieve the effect of reasonable information processing.

(iii) Different from considering the state estimation of CNNs in the sense of Lyapunov stability, this article considers the state estimation problem of CNNs in a finite-time range. The system can stay within a certain bounded range in a finite-time interval.

The rest of this article is as follows. Section 2 explains the cyberattacks, DETM, and design of the state estimator. Section 3 gives the conditions of stochastic finite-time bounded-(SFTB). Section 4 gives a numerical example to prove the correctness of the conclusion. Section 5 summarizes the full text and get conclusion.

Notation: In this article, R^n and $R^{m\times n}$ indicate the n-dimensional Euclidean space and all $m\times n$ real matrices respectively. $\mathrm{diag}_N\{\cdot\}$ and I_N represent the N-dimensional diagonal matrix and the N-dimensional identity matrix. $*$ denotes the transpose of the symmetrical position. $\otimes$ represents the Kronecker product. $\mathbb{E}\{\cdot\}$ represents the mathematical expectation.

2. Problem formulation

2.1. Coupled neural networks

Consider the following class of CNNs containing n state vectors

$$\begin{cases} x_i(k+1) = A_i x_i(k) + C_i F(x_i(k)) \\ \qquad\qquad + \sum_{j=1}^{N} \omega_{ij}\Gamma x_j(k) + B_i v(k), \\ y_i(k) = D_i x_i(k), \\ z_i(k) = N_i x_i(k), \end{cases} \tag{1}$$

where $x_i(k) \triangleq \left[\, x_{i1}(k)\ x_{i2}(k)\ \cdots\ x_{in}(k) \,\right]^{\mathrm{T}} \in R^n$ is the neural state vector. The inner-coupling matrix $\Gamma \triangleq \mathrm{diag}_n\{\tau_1,\tau_2,\ldots,\tau_n\} \geqslant 0$. The symmetric outer-coupling matrix W_ω satisfies $\omega_{ii} = -\sum_{j=1,j\neq i}^{N}\omega_{ij}$, $\omega_{ij} > 0$ $(i \neq j)$. They represent the coupling between neurons, reflecting how different parts of each other affect and interact. $y_i(k) \in R^m$ denotes the measurement output of node i. The diagonal elements in $A_i \triangleq \mathrm{diag}_n\{a_{1i},a_{2i},\ldots,a_{ni}\}$ represent specific coefficients for individual neurons. $F(x_i(k)) \triangleq \left[\, f_1(x_{i1}(k))\ f_2(x_{i2}(k))\ \cdots\ f_n(x_{in}(k)) \,\right]^{\mathrm{T}}$ denotes the nonlinear neuron activation function vector. $z_i(k) \in R^m$ is the control output of node i. $B_i \in R^{n\times h}$, $C_i \in R^{n\times n}$, $N_i \in R^{m\times n}$, $D_i \in R^{m\times n}$ are the known constants matrices that represent

linear processing of the networks. $v(k) \in R^h$ indicates the external disturbance which satisfies $\mathbb{E}\{v(k)^{\mathrm{T}} v(k)\} \leq \bar{v}, \bar{v} \geq 0$.

Assumption 1[38] In order to enhance the expression ability of CNNs, some nonlinear and continuous bounded neuron activation functions are introduced to deal with the complex practical problems of CNNs, and $f_i(0) = 0$, at this point there are upper and lower bounds $\bar{s}_i$ and $\underline{s}_i$. Thus it is possible to obtain

$$\underline{s}_i \leq \frac{f_i(u) - f_i(v)}{u - v} \leq \bar{s}_i, \tag{2}$$

where $u, v \in \mathbb{R}$ represent any two different points in the neuron activation functions.

2.2. Decentralized event-triggered mechanism

In the process of the sensor collecting information and transmitting it to the state estimator, To reduce the occupancy of channel resources and consider the respective state of each node to transmit the information reasonably, DETM is used for the measurement output in this article, and the triggering conditions are as follows:

$$\begin{aligned} k_{d+1}^i = k_d^i + \min_d \{ d | \left[y_i\left(k_d^i + d\right) - y_i\left(k_d^i\right) \right]^{\mathrm{T}} \Psi_i \\ \times \left[y_i\left(k_d^i + d\right) - y_i\left(k_d^i\right) \right] > \varsigma y_i\left(k_d^i\right)^{\mathrm{T}} \Psi_i y_i\left(k_d^i\right) \}, \end{aligned} \tag{3}$$

where $\Psi_i > 0$ is a symmetric matrix. $k \in \left[k_d^i, k_{d+1}^i\right)$ and $\varsigma \in [0,1)$. $y_i\left(k_d^i\right)$ represents the last transmitted measurement output and $y_i\left(k_d^i + d\right)$ represents the current sampling measurement output. If $y_i\left(k_d^i\right)$ and $y_i\left(k_d^i + d\right)$ satisfy inequality (3) then it means that the trigger condition has been reached and this sampling data can be transmitted, otherwise it is not be transmitted. Define an error $h_i(k) = y_i\left(k_d^i\right) - y_i(k)$, the $h_i(k)$ satisfies this trigger condition

$$h_i(k)^{\mathrm{T}} \Psi_i h_i(k) \leq \varsigma \left[y_i(k) + h_i(k) \right]^{\mathrm{T}} \Psi_i \left[y_i(k) + h_i(k) \right]. \tag{4}$$

With the DETM, the measured output can be expressed as

$$y_i(k) = y_i\left(k_d^i\right), k \in \left[k_d^i, k_{d+1}^i\right). \tag{5}$$

Remark 1 Considering that CNNs have multiple nodes, so the data information of multiple nodes needs to be transmitted. Therefore, it is necessary to use ETM to save channel resources. The ETM adopted in Ref. [39] is an overall ETM, which judges the trigger condition by combining the data information of all nodes at the same time. However, because the changes of some nodes are not obvious, the information that needs to be transmitted by these nodes having large changes and may not be accurately transmitted. Therefore, this article uses the node-based DETM. In this way, multiple sensors are used to transmit the information of each node, and the data information of each node is judged separately, and the data information can be transmitted when the transmission conditions are met. This DETM fully takes into account the multi-node characteristics of CNNs, and can more rationally save resources and transmit required data information.

2.3. Cyberattacks

It is essential to analyze cyberattacks in terms of the actual network environment. During transmission over a communication channel, one may be subjected to deception attacks with potentially unknown sequences as well as DoS attacks caused by large amounts of data messages blocking the channel. Whether these two cyberattacks are generated satisfies a stochastic Markov process. $\sigma(k) \in \phi^\sigma \triangleq \{1,2,3\}$ is a homogeneous Markov chain with completely known probability matrix and the system has three working modes: $\sigma(k) = 1$ normal operation, $\sigma(k) = 2$ deception attacks, and $\sigma(k) = 3$ DoS attacks. For example, λ_{12} represents the transition probability from normal operation to deception attacks. The remaining transition probabilities are similar, from which the following transition probability matrix can be obtained:

$$\Xi = \begin{bmatrix} \lambda_{11} & \lambda_{12} & \lambda_{13} \\ \lambda_{21} & \lambda_{22} & \lambda_{23} \\ \lambda_{31} & \lambda_{32} & \lambda_{33} \end{bmatrix}, \tag{6}$$

where $0 \leq \lambda_{\alpha\beta} \leq 1$, and $\sum_{\beta=1}^{3} \lambda_{\alpha\beta} = 1$ for all $\alpha \in \phi^\sigma$. Combining Eq. (5) and taking into account the effects of cyberattacks, the actual measured output is shown below:

$$\tilde{y}_i(k) = a_{i\sigma(k)} y_i\left(k_d^i\right) + b_{i\sigma(k)} \left(-y_i\left(k_d^i\right) + g\left(y_i\left(k_d^i\right)\right) \right), \tag{7}$$

where $g\left(y_i\left(k_d^i\right)\right)$ indicates the deception attack signal. Define

(i) $\sigma(k) = 1$, $a_{i1} = I_{m\times m}$, $b_{i1} = 0_{m\times m}$ which means that the system is working properly.

(ii) $\sigma(k) = 2$, $a_{i2} = I_{m\times m}$, $b_{i2} = I_{m\times m}$ which means that the system is under a deception attack.

(iii) $\sigma(k) = 3$, $a_{i3} = 0_{m\times m}$, $b_{i3} = 0_{m\times m}$ which means that the system is under a DoS attack.

Remark 2 Different from the network attacks modeled by two Bernoulli sequences,[40] this paper uses Markov process to simulate two different kinds of attacks on the network. Compared with Bernoulli sequence, Markov process can take into account the correlation between different states of the system and better capture the transfer relationship between states, which is not reflected by Bernoulli sequence. Secondly, Markov process can modify the state transition probability matrix according to the actual situation to flexibly adjust and extend it to better simulate the actual attack situation. Finally, Bernoulli sequences are mainly applicable to single or independent events and cannot provide long-term information about the behavior of the system. Therefore, the method adopted in this article is more reasonable.

Assumption 2[40] In a deception attack, the attacker's energy is generally limited, so the deception signal $g\left(y_i\left(k_d^i\right)\right)$ is a string of unknown signals that satisfies the following conditions:

$$\| g\left(y_i\left(k_d^i\right)\right) \|^2 \leq \| G y_i\left(k_d^i\right) \|^2, \tag{8}$$

where G denotes the upper bound of $g\left(y_i\left(k_d^i\right)\right)$ and is a constant coefficient matrix.

2.4. State estimators

Combining Eq. (1) and Eq. (7), the state estimator can be considered in the following form:

$$\begin{cases} \boldsymbol{x}_i(k+1) = A_i\boldsymbol{x}_i(k) + C_iF(\boldsymbol{x}_i(k)) + \sum_{j=1}^{N}\omega_{ij}\Gamma\boldsymbol{x}_j(k) \\ \qquad\qquad + K_{i\sigma(k)}(\tilde{y}_i(k) - D_i\boldsymbol{x}_i(k)), \\ \boldsymbol{z}_i(k) = N_i\boldsymbol{x}_i(k), \end{cases} \tag{9}$$

where the state estimator gain $K_{i\sigma(k)}$ will be designed later. To simplify the system expression, define

$$\begin{aligned} &x(k) \triangleq \mathrm{col}\left[x_1(k)\ x_2(k)\ \cdots\ x_N(k)\right], \\ &\boldsymbol{x}(k) \triangleq \mathrm{col}\left[\boldsymbol{x}_1(k)\ \boldsymbol{x}_2(k)\ \cdots\ \boldsymbol{x}_N(k)\right], \\ &F(x(k)) \triangleq \mathrm{col}\left[F(x_1(k))\ F(x_2(k))\ \cdots\ F(x_N(k))\right], \\ &\mathcal{A} \triangleq \mathrm{diag}_N\{A_1, A_2, \ldots, A_N\}, \\ &\mathcal{B} \triangleq \mathrm{col}\left[B_1\ B_2\ \cdots\ B_N\right], \\ &\mathcal{C} \triangleq \mathrm{diag}_N\{C_1, C_2, \ldots, C_N\}, \\ &\mathcal{D} \triangleq \mathrm{diag}_N\{D_1, D_2, \ldots, D_N\}, \\ &y(k_d) \triangleq \mathrm{col}\left[y_1\left(k_d^1\right)\ y_2\left(k_d^2\right)\ \cdots\ y_N\left(k_d^N\right)\right], \\ &\tilde{y}(k) \triangleq \mathrm{col}\left[\tilde{y}_1(k)\ \tilde{y}_2(k)\ \cdots\ \tilde{y}_N(k)\right], \\ &a_{\sigma(k)} \triangleq \mathrm{diag}_N\left\{a_{1\sigma(k)}, a_{2\sigma(k)}, \ldots, a_{N\sigma(k)}\right\}, \\ &\mathcal{K}_{\sigma(k)} \triangleq \mathrm{diag}_N\left\{K_{1\sigma(k)}, K_{2\sigma(k)}, \ldots, K_{N\sigma(k)}\right\}, \\ &h(k_d) \triangleq \mathrm{col}\left[h_1(k_d)\ h_2(k_d)\ \cdots\ h_N(k_d)\right], \\ &\Psi \triangleq \mathrm{diag}_N\{\Psi_1, \Psi_2, \ldots, \Psi_N\}, \\ &\mathcal{N} \triangleq \mathrm{diag}_N\{N_1, N_2, \ldots, N_N\}, \\ &z(k) \triangleq \mathrm{col}\left[z_1(k)\ z_2(k)\ \cdots\ z_N(k)\right]. \end{aligned}$$

The CNNs (1) and its actual measured output can be rewritten as

$$\begin{cases} x(k+1) = \mathcal{A}x(k) + \mathcal{C}F(x(k)) \\ \qquad\qquad + (W_\omega \otimes \Gamma)x(k) + \mathcal{B}v(k), \\ \tilde{y}(k) = \left(a_{\sigma(k)} - b_{\sigma(k)}\right)y(k_d) + b_{\sigma(k)}g(y(k_d)), \\ z(k) = \mathcal{N}x(k). \end{cases} \tag{10}$$

The state estimation system (9) can be rewritten as

$$\begin{cases} \boldsymbol{x}(k+1) = \mathcal{A}\boldsymbol{x}(k) + \mathcal{C}F(\boldsymbol{x}(k)) + (W_\omega \otimes \Gamma)\boldsymbol{x}(k) \\ \qquad\qquad + \mathcal{K}_{\sigma(k)}(\tilde{y}(k) - \mathcal{D}\boldsymbol{x}(k)), \\ \boldsymbol{z}(k) = \mathcal{N}\boldsymbol{x}(k). \end{cases} \tag{11}$$

Define $e(k) = x(k) - \boldsymbol{x}(k)$, $F(e(k)) = F(x(k)) - F(\boldsymbol{x}(k))$, the state estimation error system can be expressed as

$$\begin{cases} e(k+1) = \mathcal{A}e(k) + \mathcal{C}F(e(k)) + (W_\omega \otimes \Gamma)e(k) \\ \qquad\qquad + \mathcal{B}v(k) - \mathcal{K}_{\sigma(k)}(\tilde{y}(k) - \mathcal{D}\boldsymbol{x}(k)), \\ \tilde{z}(k) = \mathcal{N}e(k). \end{cases} \tag{12}$$

To simplify the notation, the parameters $\sigma(k)$ and $\sigma(k+1)$ are rewritten as subscript α and β. Let $\eta(k) = \mathrm{col}\left[x(k)\ e(k)\right]$, $\mathcal{F}(\eta(k)) = \mathrm{col}\left[F(x(k))\ F(e(k))\right]$, systems (10) and (12) can be further rewritten as an augmentation system

$$\begin{cases} \eta(k+1) = \Theta_{\mathcal{A}}\eta(k) + \mathcal{C}_2\mathcal{F}(\eta(k)) \\ \qquad\qquad + \mathcal{B}_2v(k) + \mathcal{H}h(k) + Yg(y(k_d)), \\ \check{z}(k) = \bar{\mathcal{N}}\eta(k), \end{cases} \tag{13}$$

where

$$\begin{aligned} &\Theta_{\mathcal{A}} \triangleq \begin{bmatrix} \mathcal{A} + W_\omega \otimes \Gamma & 0 \\ \mathcal{K}_\alpha(I_{nN} - a_\alpha + b_\alpha)\mathcal{D} & \mathcal{A} - \mathcal{K}_\alpha\mathcal{D} + W_\omega \otimes \Gamma \end{bmatrix}, \\ &\mathcal{C}_2 \triangleq \begin{bmatrix} \mathcal{C} & 0 \\ 0 & \mathcal{C} \end{bmatrix}, \\ &\mathcal{B}_2 \triangleq \begin{bmatrix} \mathcal{B} \\ \mathcal{B} \end{bmatrix}, \quad \mathcal{H} \triangleq \begin{bmatrix} 0 \\ \mathcal{K}_\alpha(b_\alpha - a_\alpha) \end{bmatrix}, \\ &Y \triangleq \begin{bmatrix} 0 \\ -\mathcal{K}_\alpha b_\alpha \end{bmatrix}, \quad \bar{\mathcal{N}} \triangleq \begin{bmatrix} 0\ \mathcal{N} \end{bmatrix}. \end{aligned}$$

Definition 1[34] The augmentation system (13) is the stochastic finite-time bounded-$(\rho_0, \rho_1, R, h, \bar{v})$, where $0 < \rho_0 < \rho_1$ and matrix $R > 0$, if $k \in \{1, 2, 3\ldots, h\}$, the following inequality holds:

$$\begin{cases} \mathbb{E}\{\eta(0)^{\mathrm{T}}R\eta(0)\} \le \rho_0, \\ \mathbb{E}\{v(k)^{\mathrm{T}}v(k)\} \le \bar{v}, \end{cases} \Rightarrow \mathbb{E}\{\eta(k)^{\mathrm{T}}R\eta(k)\} \le \rho_1. \tag{14}$$

Definition 2[34] The augmentation system (13) is the stochastic finite-time bounded-$(\rho_0, \rho_1, R, h, \bar{v})$ and satisfies the H_∞ performance index q, where $0 < \rho_0 < \rho_1$ and matrix $R > 0$, if (i) the augmentation system (13) is the stochastic finite-time bounded-$(\rho_0, \rho_1, R, h, \bar{v})$ and (ii) under zero initial state $\check{z}(k)$ satisfies

$$\mathbb{E}\left\{\sum_{k=0}^{h}\check{z}^{\mathrm{T}}(k)\check{z}(k)\right\} < q^2\mathbb{E}\left\{\sum_{k=0}^{h}v(k)^{\mathrm{T}}v(k)\right\}.$$

The primary purpose of this article is the design of state estimator which ensures the augmentation system (13) is SFTB-$(\rho_0, \rho_1, R, h, \bar{v})$.

Remark 3 In this article, SFTB is considered, which has a clear time limit and can accurately grasp the dynamic characteristics of the system in a short time. In many real CNNs state estimation problems, there will be a variety of short-term, specific time period tasks, SFTB provides a more appropriate performance guarantee for these practical scenarios. And the state estimator designed in this paper meets the H_∞ performance index, and has stronger robustness when there is external interference.

3. Main results

The SFTB-$(\rho_0, \rho_1, R, h, \bar{v})$ conditions for the augmentation system are given in this section. It can be derived from the following theorem.

Theorem 1 Given some constants $\bar{q}>0$, $h>0$, $\mu>1$, $\rho_0>0$, $\rho_1>0$, $\bar{v}>0$, $\varpi_1>0$. The augmentation system (13) is SFTB with respect to $(\rho_0,\rho_1,R,h,\bar{v})$ and satisfies an H_∞ performance indicator $q=\bar{q}\sqrt{\mu^h}$. If there exist a constant $\varpi_2>0$, block diagonal matrix $\Psi>0$, symmetric matrix $P_\alpha>0$, diagonal matrix $\Upsilon>0$ and satisfy the following conditions:

$$\begin{bmatrix} \Phi_{11} & \widetilde{L} & 0 & \Phi_{14} & 0 & \Theta_{\mathcal{A}}^{\mathrm{T}} \\ * & -\Upsilon & 0 & 0 & 0 & \mathcal{C}_2^{\mathrm{T}} \\ * & * & -\bar{q}^2 I & 0 & 0 & \mathcal{B}_2^{\mathrm{T}} \\ * & * & * & \Phi_{44} & 0 & \mathcal{H}^{\mathrm{T}} \\ * & * & * & * & -I_g & Y^{\mathrm{T}} \\ * & * & * & * & * & -\tilde{P}_\beta^{-1} \end{bmatrix} < 0, \tag{15}$$

$$\begin{bmatrix} -P_\alpha & \sqrt{\varpi_1} IR \\ * & -R \end{bmatrix} < 0, \tag{16}$$

$$\begin{bmatrix} -\varpi_2 R & P_\alpha \\ * & -P_\alpha \end{bmatrix} < 0, \tag{17}$$

$$\varpi_1^{-1}\mu^h\left[\varpi_2\rho_0+\frac{\bar{q}^2\bar{v}}{\mu-1}\right]\le\rho_1, \tag{18}$$

where

$$\begin{aligned} \tilde{P}_\beta &\triangleq \sum_{\beta\in\phi^\sigma}\lambda_{\alpha\beta}P_\beta,\ \Psi\triangleq \mathrm{diag}_N\{\Psi_1,\Psi_2,\ldots,\Psi_N\},\\ \Phi_{11} &\triangleq -\mu P_\alpha-\widehat{L}+\mathcal{N}^{\mathrm{T}}\mathcal{N}\\ &\quad+\begin{bmatrix} I \\ 0 \end{bmatrix}\left(\mathcal{D}^{\mathrm{T}}G^{\mathrm{T}}G\mathcal{D}+\varsigma\mathcal{D}^{\mathrm{T}}\Psi\mathcal{D}\right)\begin{bmatrix} I & 0 \end{bmatrix},\\ \Phi_{14} &\triangleq \varsigma\begin{bmatrix} I \\ 0 \end{bmatrix}\mathcal{D}^{\mathrm{T}}\Psi+\begin{bmatrix} I \\ 0 \end{bmatrix}\mathcal{D}^{\mathrm{T}}G^{\mathrm{T}}G,\\ \Phi_{44} &\triangleq (\varsigma-1)\Psi+G^{\mathrm{T}}G. \end{aligned}$$

Proof For the augmentation system (13) chooses the following Lyapunov function:

$$V(k)=\eta(k)^{\mathrm{T}}P_\alpha\eta(k), \tag{19}$$

then, let $\mathcal{Q}(k)=\mathrm{col}\left[\eta(k)\ \mathcal{F}(\eta(k))\ v(k)\ h(k)\ g(y(k_d))\right]$, $\mathcal{W}=\left[\Theta_{\mathcal{A}}\ \mathcal{C}_2\ \mathcal{B}_2\ \mathcal{H}\ Y\right]$, $\mathbb{E}\{\Delta V(k)\}$ can be written as

$$\begin{aligned} \mathbb{E}\{\Delta V(k)\} &= \mathbb{E}\{V(k+1)\}-\mu V(k)\\ &= \eta(k+1)^{\mathrm{T}}\sum_{\beta\in\phi^\sigma}\lambda_{\alpha\beta}P_\beta\eta(k+1)\\ &\quad-\mu\eta(k)^{\mathrm{T}}P_\alpha\eta(k)\\ &= \mathcal{Q}(k)^{\mathrm{T}}\mathcal{W}^{\mathrm{T}}\tilde{P}_\beta\mathcal{W}\mathcal{Q}(k)-\mu\eta(k)^{\mathrm{T}}P_\alpha\eta(k). \end{aligned} \tag{20}$$

From Assumption 1, it follows that

$$\begin{bmatrix} \eta_{ij}(k) \\ \mathcal{F}_j(\eta_{ij}(k)) \end{bmatrix}^{\mathrm{T}}\begin{bmatrix} \varepsilon_i\bar{s}_i\underline{s}_i & -\varepsilon_i\frac{\bar{s}_i+\underline{s}_i}{2} \\ * & \varepsilon_i \end{bmatrix}\begin{bmatrix} \eta_{ij}(k) \\ \mathcal{F}_j(\eta_{ij}(k)) \end{bmatrix}\le 0,$$

where $\varepsilon_i>0$, $i\triangleq\{1,2,3,\ldots,n\}$, $j\triangleq\{1,2,3,\ldots,N\}$. Expanding the dimension of the above matrix yields

$$\left[\eta(k)^{\mathrm{T}}\ \mathcal{F}(\eta(k))^{\mathrm{T}}\right]\begin{bmatrix} \widehat{L} & -\widetilde{L} \\ * & \Upsilon \end{bmatrix}\begin{bmatrix} \eta(k) \\ \mathcal{F}(\eta(k)) \end{bmatrix}\le 0, \tag{21}$$

where

$$\begin{aligned} &\widehat{L}\triangleq \mathrm{diag}_N\left\{\bar{\varepsilon}\hat{l},\bar{\varepsilon}\hat{l},\ldots,\bar{\varepsilon}\hat{l}\right\},\\ &\widetilde{L}\triangleq \mathrm{diag}_N\left\{\bar{\varepsilon}\tilde{l},\bar{\varepsilon}\tilde{l},\ldots,\bar{\varepsilon}\tilde{l}\right\},\\ &\hat{l}\triangleq \mathrm{diag}\left\{\bar{s}_1\underline{s}_1,\bar{s}_2\underline{s}_2,\ldots,\bar{s}_n\underline{s}_n\right\},\\ &\tilde{l}\triangleq \mathrm{diag}\left\{\frac{\bar{s}_1+\underline{s}_1}{2},\frac{\bar{s}_2+\underline{s}_2}{2},\ldots,\frac{\bar{s}_n+\underline{s}_n}{2}\right\},\\ &\Upsilon\triangleq \mathrm{diag}_N\{\bar{\varepsilon},\bar{\varepsilon},\ldots,\bar{\varepsilon}\},\quad \bar{\varepsilon}\triangleq\mathrm{diag}\{\varepsilon_1,\varepsilon_2,\ldots,\varepsilon_n\}. \end{aligned}$$

From Assumption 2, it follows that

$$y(k_d)^{\mathrm{T}}G^{\mathrm{T}}Gy(k_d)-g(y(k_d))^{\mathrm{T}}g(y(k_d))\ge 0. \tag{22}$$

It follows from inequality (4) that

$$\varsigma[y(k)+h(k)]^{\mathrm{T}}\Psi[y(k)+h(k)]-h(k)^{\mathrm{T}}\Psi h(k)\ge 0. \tag{23}$$

According to the constructed Lyapunov function one obtains

$$V(k)\ge\lambda_{\min}\left(R^{-1/2}P_\alpha R^{-1/2}\right)\eta(k)^{\mathrm{T}}R\eta(k). \tag{24}$$

According to Eq. (20) it is possible to obtain

$$\begin{aligned} &\mathbb{E}\{\Delta V(k)\}-\bar{q}^2v(k)^{\mathrm{T}}v(k)+\breve{z}^{\mathrm{T}}(k)\breve{z}(k)\\ &=\mathbb{E}\{V(k+1)\}-\mu V(k)+\breve{z}^{\mathrm{T}}(k)\breve{z}(k)-\bar{q}^2v(k)^{\mathrm{T}}v(k), \end{aligned} \tag{25}$$

due to $\mathbb{E}\left\{v(k)^{\mathrm{T}}v(k)\right\}\le\bar{v}$ for all $k\in\{1,2,\ldots,h\}$, $\eta(0)^{\mathrm{T}}R\eta(0)<\rho_0$. One can get that from Eq. (25)

$$\begin{aligned} V(k) &< \mu^kV(0)+\bar{q}^2\sum_{\gamma=0}^{k-1}\mu^{k-1-\gamma}v(k)^{\mathrm{T}}v(k)\\ &\quad-\sum_{\gamma=0}^{k-1}\mu^{k-1-\gamma}\breve{z}^{\mathrm{T}}(k)\breve{z}(k)\\ &< \mu^kV(0)+\bar{q}^2\bar{v}\frac{\mu^k-1}{\mu-1}\\ &< \mu^k\left[\lambda_{\max}\left(R^{-1/2}P_\alpha R^{-1/2}\right)\eta(0)^{\mathrm{T}}R\eta(0)+\bar{q}^2\bar{v}\frac{1}{\mu-1}\right]\\ &< \mu^h\left[\lambda_{\max}\left(R^{-1/2}P_\alpha R^{-1/2}\right)\rho_0+\bar{q}^2\bar{v}\frac{1}{\mu-1}\right]. \end{aligned}$$

Combined with Schur's complement, from inequalities (16) and (17) we can obtain

$$\varpi_1 I<R^{-1/2}P_\alpha R^{-1/2}<\varpi_2 I. \tag{26}$$

From expressions (25) and (24) we can get

$$\eta(k)^{\mathrm{T}}R\eta(k)<\varpi_1^{-1}\mu^h\left[\varpi_2\rho_0+\frac{\bar{q}^2\bar{v}}{\mu-1}\right]\le\rho_1. \tag{27}$$

Thus by Definition 1, it is known that the system is SFTB with respect to$(\rho_0,\rho_1,R,h,\bar{v})$.

In addition, the zero initial condition can be obtained $V(0)=0$, $V(k)>0$. From the above derivation it follows that

$$V(k)<\bar{q}^2\sum_{\gamma=0}^{k-1}\mu^{k-1-\gamma}v(k)^{\mathrm{T}}v(k)-\sum_{\gamma=0}^{k-1}\mu^{k-1-\gamma}\breve{z}(k)^{\mathrm{T}}\breve{z}(k)$$

$$< \mu^h \bar{q}^2 \sum_{\gamma=0}^{k-1} v(k)^{\mathrm{T}} v(k) - \sum_{\gamma=0}^{k-1} \breve{z}^{\mathrm{T}}(k) \breve{z}(k),$$

since $\mu > 1$, it follows that

$$\sum_{k=0}^{h} \breve{z}^{\mathrm{T}}(k) \breve{z}(k) < q^2 \sum_{k=0}^{h} v(k)^{\mathrm{T}} v(k),$$

where $q = \bar{q}\sqrt{\mu^h}$. Thus the H_∞ performance index q is satisfied. Proof of completion at this point.

Theorem 2 Given constants $\bar{q} > 0$, $h > 0$, $\mu > 1$, $\rho_0 > 0$, $\rho_1 > 0$, $\bar{v} > 0$, $\varpi_1 > 0$. The augmentation system (13) is SFTB with respect to $(\rho_0, \rho_1, R, h, \bar{v})$ and satisfies an H_∞ performance indicator $q = \bar{q}\sqrt{\mu^h}$. If there exist a constant $\varpi_2 > 0$, several block diagonal matrices $\Psi > 0$, Λ_α, Π_α, symmetric matrix $P_\alpha > 0$, and diagonal matrix $\Upsilon > 0$ satisfying inequalities (16)–(18) and the following conditions:

$$\begin{bmatrix} \Phi_{11} & \widetilde{L} & 0 & \Phi_{14} & 0 & \Theta_{\mathcal{A}}^{\mathrm{T}} \Omega_\alpha^{\mathrm{T}} \\ ** & -\Upsilon & 0 & 0 & 0 & \mathcal{C}_2^{\mathrm{T}} \Omega_\alpha^{\mathrm{T}} \\ ** & * & -\bar{q}^2 I & 0 & 0 & \mathcal{B}_2^{\mathrm{T}} \Omega_\alpha^{\mathrm{T}} \\ ** & * & * & \Phi_{44} & 0 & \mathcal{H}^{\mathrm{T}} \Omega_\alpha^{\mathrm{T}} \\ ** & * & * & * & -I_g & Y^{\mathrm{T}} \Omega_\alpha^{\mathrm{T}} \\ ** & * & * & * & * & \Phi_{66} \end{bmatrix} < 0, \tag{28}$$

where

$$\Phi_{66} = \tilde{P}_\beta - \Omega_\alpha - \Omega_\alpha^{\mathrm{T}}, \quad \Omega_\alpha = \begin{bmatrix} \Lambda_\alpha & 0 \\ 0 & \Lambda_\alpha \end{bmatrix},$$
$$\Psi \triangleq \mathrm{diag}_N \{\Psi_1, \Psi_2, \ldots, \Psi_N\},$$
$$\Lambda_\alpha \triangleq \mathrm{diag}_N \{V_{1\alpha}, V_{2\alpha}, \ldots, V_{N\alpha}\},$$
$$\Pi_\alpha \triangleq \mathrm{diag}_N \{M_{1\alpha}, M_{2\alpha}, \ldots, M_{N\alpha}\},$$

then the state estimator gain $K_{i\alpha} = V_{i\alpha}^{-1} M_{i\alpha}$.

Proof According to the inequality

$$\left(\tilde{P}_\beta - \Omega_\alpha\right) \tilde{P}_\beta^{-1} \left(\tilde{P}_\beta - \Omega_\alpha^{\mathrm{T}}\right) \geq 0,$$

thus it can be obtained

$$\tilde{P}_\beta - \Omega_\alpha - \Omega_\alpha^{\mathrm{T}} \geq -\Omega_\alpha \tilde{P}_\beta^{-1} \Omega_\alpha^{\mathrm{T}}. \tag{29}$$

According to inequalities (28) and (29) we get

$$\begin{bmatrix} \Phi_{11} & \widetilde{L} & 0 & \Phi_{14} & 0 & \Theta_{\mathcal{A}}^{\mathrm{T}} \Omega_\alpha^{\mathrm{T}} \\ ** & -\Upsilon & 0 & 0 & 0 & \mathcal{C}_2^{\mathrm{T}} \Omega_\alpha^{\mathrm{T}} \\ ** & * & -\bar{q}^2 I & 0 & 0 & \mathcal{B}_2^{\mathrm{T}} \Omega_\alpha^{\mathrm{T}} \\ ** & * & * & \Phi_{44} & 0 & \mathcal{H}^{\mathrm{T}} \Omega_\alpha^{\mathrm{T}} \\ ** & * & * & * & -I_g & Y^{\mathrm{T}} \Omega_\alpha^{\mathrm{T}} \\ ** & * & * & * & * & -\Omega_\alpha \tilde{P}_\beta^{-1} \Omega_\alpha^{\mathrm{T}} \end{bmatrix} < 0. \tag{30}$$

By multiplying both sides of the matrix (30) by the diagonal matrix $\mathrm{diag}\{I, I, I, I, I, \Omega_\alpha^{-1}\}$ and $\mathrm{diag}\{I, I, I, I, I, \Omega_\alpha^{-\mathrm{T}}\}$, which implies inequality (15). According to inequalities (16)–(18) and (28), it can be obtained that the augmentation system is SFTB-$(\rho_0, \rho_1, R, h, \bar{v})$.

Remark 4 According to Definition 1, it can be seen that if ρ_0 is given constants and the initial state of the system is set to be less than given constant. This article deals with SFTB, so in a finite period of time, the state trajectories of the system will be less than a certain threshold, that is, ρ_1. Then, the value of ρ_1 in the experiment involves a problem of parameter optimization. In this article, the minimum value algorithm is adopted to find the minimum value of ρ_1, and its minimum value is adopted in the subsequent experiment, which can reduce the conservatism of the experiment and make the experiment effect better.

4. An illustrative example

Considering the feasibility of the results, this section gives a numerical example to demonstrate the results. Analyze the four operating states of the three nodes of the system: system working normally, system suffering from deception attack, system suffering from DoS attack, and system suffering from mixed cyberattacks. Given the following parameters for the three nodes of the system

$$A_1 = \begin{bmatrix} 0.55 & 0 \\ 0 & 0.52 \end{bmatrix}, \quad C_1 = \begin{bmatrix} 0.4 & 0.3 \\ 0.3 & 0.2 \end{bmatrix}, \quad B_1 = \begin{bmatrix} 0.05 \\ 0.04 \end{bmatrix},$$
$$D_1 = \begin{bmatrix} 0.85 & 0.90 \end{bmatrix}, \quad N_1 = \begin{bmatrix} 0.50 & 0.30 \end{bmatrix},$$
$$A_2 = \begin{bmatrix} 0.51 & 0 \\ 0 & 0.50 \end{bmatrix}, \quad C_2 = \begin{bmatrix} 0.3 & 0.3 \\ 0.2 & 0.4 \end{bmatrix}, \quad B_2 = \begin{bmatrix} 0.05 \\ 0.06 \end{bmatrix},$$
$$D_2 = \begin{bmatrix} 0.80 & 0.80 \end{bmatrix}, \quad N_2 = \begin{bmatrix} 0.45 & 0.50 \end{bmatrix},$$
$$A_3 = \begin{bmatrix} 0.52 & 0 \\ 0 & 0.60 \end{bmatrix}, \quad C_3 = \begin{bmatrix} 0.2 & 0.2 \\ 0.2 & 0.3 \end{bmatrix}, \quad B_3 = \begin{bmatrix} 0.04 \\ 0.03 \end{bmatrix},$$
$$D_3 = \begin{bmatrix} 0.90 & 0.80 \end{bmatrix}, \quad N_3 = \begin{bmatrix} 0.50 & 0.40 \end{bmatrix}.$$

The transfer probabilities for the four operating states are shown in Table 1. The out-coupling matrix for the three nodes is given as follows:

$$W_\omega = \begin{bmatrix} -0.4 & 0.2 & 0.2 \\ 0.2 & -0.4 & 0.2 \\ 0.2 & 0.2 & -0.4 \end{bmatrix}.$$

The inner-coupling matrix for three nodes is expressed as

$$\Gamma = \begin{bmatrix} 0.5 & 0 \\ 0 & 0.3 \end{bmatrix}.$$

The neuron activation function and deception attacks function is defined as

$$F(x_i(k)) = 0.1\left(|(x_i(k)+1)| - |(x_i(k)-1)|\right),$$
$$g\left(y_i\left(k_d^i\right)\right) = -2\tanh\left(y_i\left(k_d^i\right)\right), i \in \{1, 2, 3\},$$

where $\rho_0 = 0.1$, $\mu = 1.01$, $\varsigma = 0.01$, $\varpi_1 = 1.01$, $h = 40$, $\bar{q} = 1.3$, $\bar{v} = 0.01$ and R is the identity matrix of appropriate dimensions. According to Remark 4, $\min(\rho_1) = 4.3861$, The external disturbance $v(k) = 0.1\sin(0.8k)\,\mathrm{e}^{-0.1k}$.

Table 1. Transfer probability matrix for different operating states.

Case I: normal operation	Case II: deception attacks	Case III: DoS attacks	Case IV: hybrid cyberattacks
$\Xi_1=\begin{bmatrix}1&0&0\\1&0&0\\1&0&0\end{bmatrix}$	$\Xi_2=\begin{bmatrix}0.7&0.3&0\\0.7&0.3&0\\0.6&0.4&0\end{bmatrix}$	$\Xi_3=\begin{bmatrix}0.7&0&0.3\\0.7&0&0.3\\0.6&0&0.4\end{bmatrix}$	$\Xi_4=\begin{bmatrix}0.7&0.1&0.2\\0.7&0.2&0.1\\0.6&0.2&0.2\end{bmatrix}$

According to Theorem 2 and Table 1, when the system is in the case I, the state estimator gains are as follows:

$$K_{11}=\begin{bmatrix}0.3158\\0.2527\end{bmatrix},\quad K_{12}=\begin{bmatrix}-0.0339\\-0.0270\end{bmatrix},$$
$$K_{13}=\begin{bmatrix}-0.0339\\-0.0270\end{bmatrix},$$
$$K_{21}=\begin{bmatrix}0.4964\\0.5893\end{bmatrix},\quad K_{22}=\begin{bmatrix}-0.0597\\-0.0710\end{bmatrix},$$
$$K_{23}=\begin{bmatrix}-0.0599\\-0.0712\end{bmatrix},$$
$$K_{31}=\begin{bmatrix}0.2995\\0.2247\end{bmatrix},\quad K_{32}=\begin{bmatrix}-0.0323\\-0.0242\end{bmatrix},$$
$$K_{33}=\begin{bmatrix}-0.0324\\-0.0242\end{bmatrix}.$$

When the system is in the case II, the state estimator gains are as follows:

$$K_{11}=\begin{bmatrix}0.3157\\0.2530\end{bmatrix},\quad K_{12}=\begin{bmatrix}-0.0351\\-0.0281\end{bmatrix},$$
$$K_{13}=\begin{bmatrix}-0.0339\\-0.0271\end{bmatrix},$$
$$K_{21}=\begin{bmatrix}0.4907\\0.5831\end{bmatrix},\quad K_{22}=\begin{bmatrix}-0.0552\\-0.0656\end{bmatrix},$$
$$K_{23}=\begin{bmatrix}-0.0593\\-0.0706\end{bmatrix},$$
$$K_{31}=\begin{bmatrix}0.2992\\0.2250\end{bmatrix},\quad K_{32}=\begin{bmatrix}-0.0333\\-0.0250\end{bmatrix},$$
$$K_{33}=\begin{bmatrix}-0.0324\\-0.0243\end{bmatrix}.$$

When the system is in the case III, the state estimator gains are as follows:

$$K_{11}=\begin{bmatrix}0.3157\\0.2529\end{bmatrix},\quad K_{12}=\begin{bmatrix}-0.0339\\-0.0271\end{bmatrix},$$
$$K_{13}=\begin{bmatrix}-0.0352\\-0.0281\end{bmatrix},$$
$$K_{21}=\begin{bmatrix}0.4938\\0.5868\end{bmatrix},\quad K_{22}=\begin{bmatrix}-0.0593\\-0.0706\end{bmatrix},$$
$$K_{23}=\begin{bmatrix}-0.0550\\-0.0654\end{bmatrix},$$
$$K_{31}=\begin{bmatrix}0.2991\\0.2247\end{bmatrix},\quad K_{32}=\begin{bmatrix}-0.0324\\-0.0243\end{bmatrix},$$
$$K_{33}=\begin{bmatrix}-0.0334\\-0.0250\end{bmatrix}.$$

When the system is in the case IV, the state estimator gains are as follows:

$$K_{11}=\begin{bmatrix}0.3156\\0.2529\end{bmatrix},\quad K_{12}=\begin{bmatrix}-0.0350\\-0.0280\end{bmatrix},$$
$$K_{13}=\begin{bmatrix}-0.0351\\-0.0280\end{bmatrix},$$
$$K_{21}=\begin{bmatrix}0.4907\\0.5832\end{bmatrix},\quad K_{22}=\begin{bmatrix}-0.0555\\-0.0660\end{bmatrix},$$
$$K_{23}=\begin{bmatrix}-0.0551\\-0.0656\end{bmatrix},$$
$$K_{31}=\begin{bmatrix}0.2990\\0.2249\end{bmatrix},\quad K_{32}=\begin{bmatrix}-0.0332\\-0.0249\end{bmatrix},$$
$$K_{33}=\begin{bmatrix}-0.0333\\-0.0250\end{bmatrix}.$$

Assume that the initial state is

$$x_1(0)=\begin{bmatrix}0.1\\0.15\end{bmatrix},\quad x_2(0)=\begin{bmatrix}0.2\\0.1\end{bmatrix},\quad x_3(0)=\begin{bmatrix}0.1\\0.2\end{bmatrix},$$
$$\boldsymbol{x}_1(0)=\begin{bmatrix}0\\0\end{bmatrix},\quad \boldsymbol{x}_2(0)=\begin{bmatrix}0\\0\end{bmatrix},\quad \boldsymbol{x}_3(0)=\begin{bmatrix}0\\0\end{bmatrix}.$$

From the above conditions it can be easily obtained $\mathbb{E}\{v(k)^{\mathrm{T}}v(k)\}\leq\bar{v}$, $\eta(0)^{\mathrm{T}}R\eta(0)\leq\rho_0$. Since the cyberattacks in the estimation system of this article are stochastic, 500 experiments are simulated to find the estimation error of the system in Figs. 2–5 to avoid randomness.

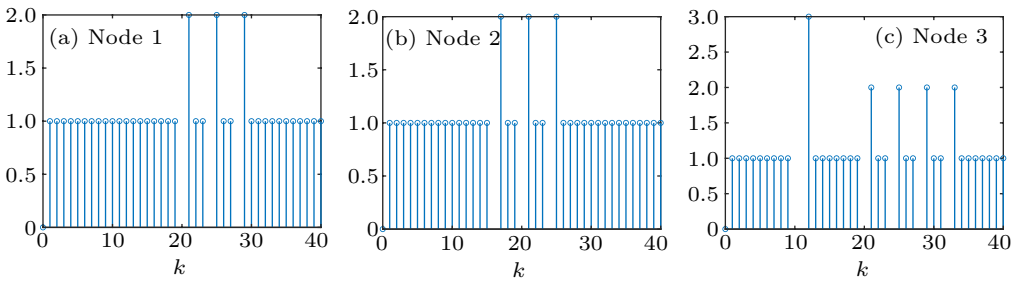


Fig. 1. Trigger sequence of three nodes.

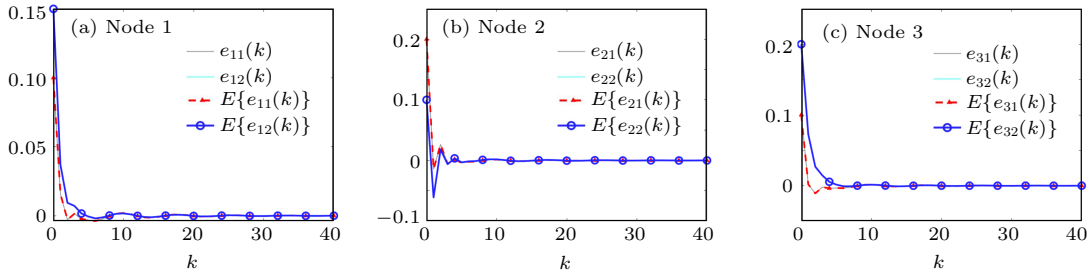


Fig. 2. Estimation error of three nodes in normal operation.

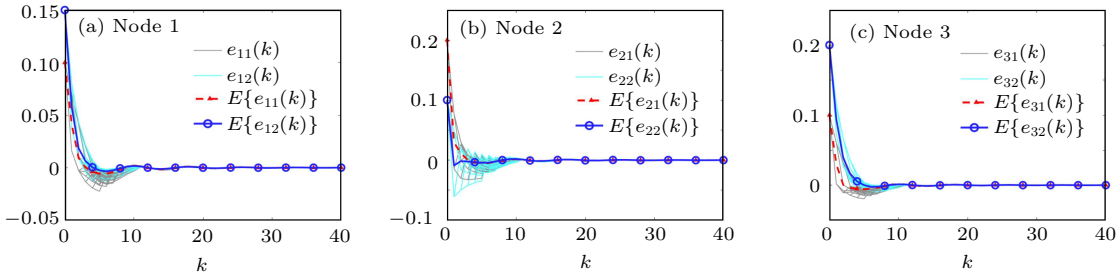


Fig. 3. Estimation error of three nodes under deception attacks.

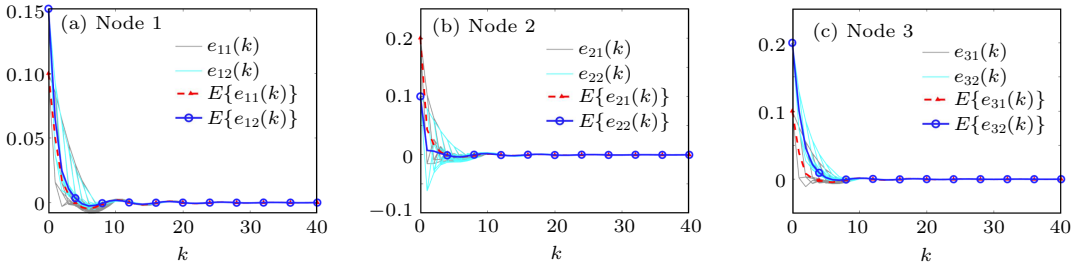


Fig. 4. Estimation error of three nodes under DoS attacks.

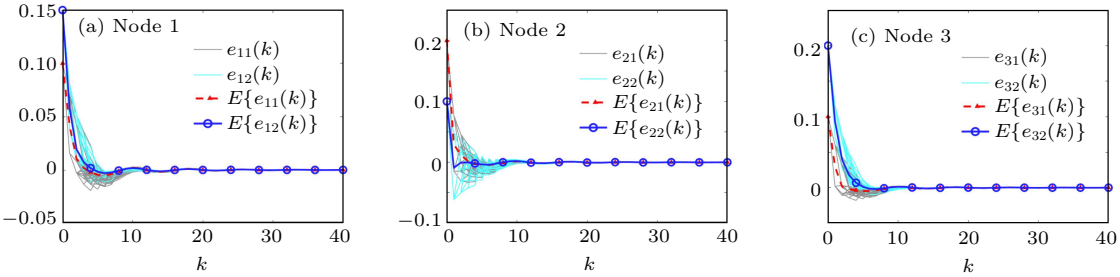


Fig. 5. Estimation error of three nodes under mixed cyberattacks.

In Fig. 1, from left to right is the trigger sequence diagram of node one to node three, due to the DETM, the trigger moment of each node is based on the actual state of each node to determine whether to trigger or not, so the trigger moment will be different.

In Fig. 2, when $k = 20$, the estimation error of node 1 is equal to 0; when $k = 20$, the estimation error of node 2 is zero; when $k = 15$, the estimation error of node 3 is also 0. It can be seen that after these moments, the state trajectory of the estimation system has coincided with that of the original system, as well as achieving the desired estimation effect. In this article, the system parameters are not related to the modal state, so when the system works completely normally, the 500 experimental results of the error system are completely coincident with its expected curve, so we can only see the two lines after the coincidence in the figure. In Figs. 3–5, it can be seen that the error may be different at the same moment in each experiment because the system may suffer from random cyberattacks. Observing the expected error it can be obtained that the error of each node is 0 after a certain moment, and all of them achieve a better estimation.

In Fig. 6, the trajectories are all zero after $k = 10$. It can be seen that the system in either operating state satisfies $\eta(k)^{\mathrm{T}} R\eta(k) \leq \min(\rho_1)$, which shows the system satisfies the finite-time threshold condition that indicates the system is SFTB-$(\rho_0, \rho_1, R, h, \bar{v})$.

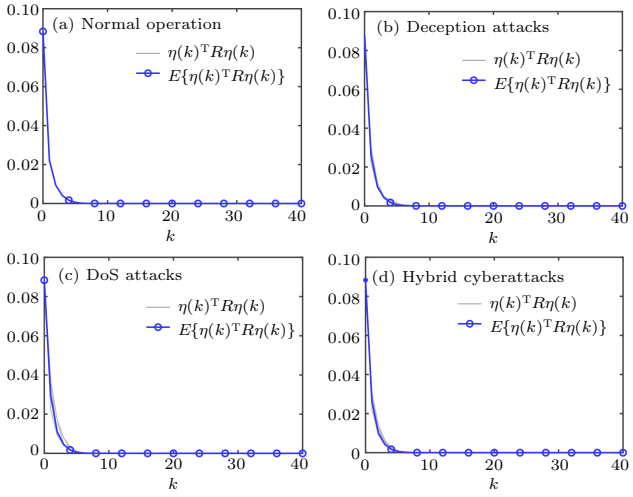


Fig. 6. State trajectories of $\eta(k)^{\mathrm{T}}R\eta(k)$ in four operating states.

5. Conclusions

This article has studied the finite-time state estimation problem of CNNs under unreliable Markovian network against mixed cyberattacks. Under the condition of SFTB-$(\rho_0,\rho_1,R,h,\bar{v})$, the Markov process is used to establish the design strategy of state estimators in different working modes under cyberattacks. Combining with the DETM, the Lyapunov function is constructed to get sufficient conditions for the design of the state estimator. By solving the LMIs, the necessary and appropriate gain of state estimator is obtained so that the coupled neural network can achieve the finite-time state estimation under the H_∞ performance index. Finally, a numerical example is given to prove the effectiveness and feasibility of the proposed method.

Acknowledgements

Project supported by the National Natural Science Foundation of China (Grant No. 62303016), the Research and Development Project of Engineering Research Center of Biofilm Water Purification and Utilization Technology of the Ministry of Education of China (Grant No. BWPU2023ZY02), the University Synergy Innovation Program of Anhui Province, China (Grant No. GXXT-2023-020), and the Key Project of Natural Science Research in Universities of Anhui Province, China (Grant No. 2024AH050171).

References

[1] Storm L, Linander H, Bec J, Gustavsson K and Mehlig B 2024 *Phys. Rev. Lett.* **132** 057301
[2] Louppe G, Cho K, Becot C and Cranmer K 2019 *J. High Energy Phys.* **2019** 57
[3] Ye S, Li B, Li Q, Zhao H P and Feng X Q 2019 *Appl. Phys. Lett.* **115** 161901
[4] Eckmann J P, Feinerman O, Gruendlinger L, Moses E, Soriano J and Tlusty T 2007 *Phys. Rep.* **449** 54
[5] Nubert J, Köhler J, Berenz V, Allgöwer F and Trimpe S 2020 *IEEE Rob. Autom.* **5** 3050
[6] Altan A, Karasu S and Zio E 2021 *Appl. Soft Comput.* **100** 106996
[7] Nam J, Yong H, Hwang J and Choi J 2021 *Phys. Lett. A* **387** 127005
[8] Zeng W, Yuan J, Yuan C, Wang Q, Liu F and Wang Y 2021 *Soft Comput.* **25** 4571
[9] Zhao Y and Han J 2024 *Physica D* **462** 134130
[10] Subashini M M and Sahoo S K 2014 *Expert Syst. Appl.* **41** 3965
[11] Yue J, Li J, Zhang W and Chen Z 2023 *Chin. Phys. B* **32** 010201
[12] Xing J, Wu W, Cheng Q and Liu R 2022 *Physica A* **595** 127079
[13] Cao J and Li L 2009 *Neural Netw.* **22** 335
[14] Liu Y, Shen B and Zhang P 2022 *Neural Netw.* **150** 181
[15] Wang G, Shen Y and Yin Q 2013 *Chin. Phys. B* **22** 050504
[16] Chen Y, Meng X, Wang Z and Dong H 2021 *IEEE Trans. Neural Netw. Learn. Syst.* **34** 1465
[17] Zhu S, Bao H and Cao J 2022 *Physica A* **600** 127586
[18] Shao H Y, Hu A H and Liu D 2015 *Chin. Phys. B* **24** 098902
[19] Xu Z, Liu X Z, Chen Q W and Wu Z X 2020 *Chin. Phys. B* **29** 050701
[20] Liu S, Wang Z, Chen Y and Wei G 2020 *Neural Netw.* **132** 211
[21] Senan S, Ali M S, Vadivel R and Arik S 2017 *Neural Netw.* **86** 32
[22] Huang W, Zhang T and Yao X 2022 *Physica A* **592** 126837
[23] Yuan H, Xia Y and Yang H 2021 *IEEE Trans. Syst. Man, Cybern. Syst.* **51** 6926
[24] Hou N, Wang Z, Ho D W and Dong H 2020 *IEEE Trans. Cybern.* **50** 2793
[25] Liu Y, Zhang P, Lee S and Xie X 2024 *IEEE Trans. Fuzzy Syst.* **32** 2438
[26] Zhao X, Liu C and Tian E 2020 *ISA Trans.* **104** 93
[27] Zhang Z Z, Xu W J, Zeng S Y and Lin J R 2014 *Chin. Phys. B* **23** 088902
[28] Kazemy A, Saravanakumar R and Lam J 2021 *Inf. Sci.* **560** 20
[29] Oliveira P M, Palma J M and Lacerda M J 2024 *IEEE Trans. Circuits Syst. II, Exp. Briefs* **71** 732
[30] Luo H, Wang Y J, Ye W, Zhong H, Mao Y Y and Guo Y 2022 *Chin. Phys. B* **31** 020306
[31] Yang X, Cao J and Lu J 2013 *IEEE Trans. Circuits Syst. I, Reg. Papers* **60** 363
[32] Zhong X, He H, Zhang H and Wang Z 2015 *Neurocomputing* **149** 116
[33] Yang X, Feng Z, Feng J and Cao J 2017 *Neural Netw.* **85** 157
[34] Dong J, Ma X, Zhang X, Zhou J and Wang Z 2023 *Chin. Phys. B* **32** 110202
[35] Wang Y, Arumugam A, Liu Y and Alsaadi F E 2020 *Neurocomputing* **384** 115
[36] Wang Z, Xu Y, Lu R and Peng H 2017 *IEEE Trans. Neural Netw. Learn. Syst.* **28** 630
[37] Xi Y, Yu Y, Zhang S and Hai X 2018 *Chin. Phys. B* **27** 010202
[38] Zhao Z, Wang Z, Zou L and Guo G 2021 *IEEE Trans. Syst. Man, Cybern. Syst.* **51** 441
[39] Chen W, Shi D, Wang J and Shi L 2017 *IEEE Trans. Control Syst. Technol.* **25** 1865
[40] Zhang Z, Chen Z, Sheng Z, Li D and Wang J 2022 *Appl. Math. Comput.* **430** 127274